doi.org/10.36721/PJPS.2022.35.4.SP.1241-1250.1

3-substituted coumarin derivatives over-activate the HslV protease: A potential drug target for antibacterial activity

Sana Aurangzeb[1], Mehwish Hamid[1], Uzma Salar[2], Yasmeen Rashid[1], Khalid Mohammed Khan[2,3], M. Kamran Azim[4] and Shahid Bashir[5]

[1]Department of Biochemistry, University of Karachi, Karachi, Pakistan
[2]HEJ Research Institute of Chemistry, International Center for Chemical and Biological Sciences, University of Karachi, Karachi
[3]Department of Clinical Pharmacy, Institute for Research and Medical Consultations (IRMC), Imam Abdulrahman Bin Faisal University, Dammam, Saudi Arabia
[4]Department of Biosciences, Mohammad Ali Jinnah University, Karachi, Pakistan
[5]Neuroscience Center, King Fahad Specialist Hospital, Dammam, Saudi Arabia

Abstract: The bacterial HslVU complex consists of two different proteins, i.e., the HslV protease and the HslU ATPase. The functional HslVU enzyme complex forms only when the HslU c-terminal helix is inserted into the cavity located between two adjacent HslV monomers in order to allosterically activate the HslV protease. Based on its essential role in maintaining microbial proteostasis as well its absence from human beings, it is considered a promising therapeutic target for designing antibacterial agents. The goal of the present study was to find out potential drug candidates that could over-activate the HslV protease and produce aberrant proteolysis in pathogenic bacteria. Derivatives of 3-substituted coumarin have been identified as potential HslV protease activators based on their highest docking scores, ideal interaction patterns, and significant in-vitro HslV activation potential. Their ED^{50} values were in the sub-micromolar range, i.e., 0.4-0.48µM. The conformational stability of the contacts between the HslV dimer and the active compounds was further confirmed by molecular dynamics studies. Correspondingly, the ADMET characteristics of these lead molecules considerably demonstrated their significant non-toxic drug-like abilities. This research not only identified small non-peptidic HslV protease activators but also improved the understanding of the mode of action of 3-substituted coumarin derivatives as antibacterials.

Keywords: 3-substituted coumarin derivatives, the HslVU complex, structural bioinformatics, molecular docking studies, antimicrobial drugs.

INTRODUCTION

Prokaryotic cells contain many energy-dependent proteases including the HslVU complex in order to maintain a healthy cellular proteome. The HslVU complex is primarily found in prokaryotic cells, however, it has also been identified in some pathogenic eukaryotes (Missiakas *et al*., 1996; Barboza *et al*., 2012; Kebe *et al*., 2019). The HslVU complex consists of HslV dodecamer flanked by HslU hexamers (fig. 1A) (Sousa *et al*., 2000). The HslV dodecamer is a proteolytic chamber harboring 12 active sites whose catalytic residues are the N-terminal Threonine (Thr-1) of each subunit. The catalytic activity of the HslV protease is allosterically activated by HslU ATPase, which is also responsible for the recognition, unfolding, and translation of substrate into the proteolytic chamber by an energy-dependent mechanism (Azim, 2021).

The HslV protease alone is known to degrade some hydrophobic peptides and unfolded protein in-vitro, however, its proteolytic activity can be increased several-fold by binding with HslU ATPase (Yoo *et al*., 1996; Azim *et al*., 2005; Park *et al*., 2008). Crystallographic and mutational studies have shown that the functional HslVU complex is formed when the c-terminal helix of HslU distends and intercalates into the cleft between adjacent HslV subunits (Sousa *et al*., 2000; Seong *et al*., 2002). Notably, it has been observed that synthetic peptides composed of 8-12 amino acid residues of HslUc-tail can activate the HslV peptidase activity towards small fluorogenic peptide substrates or unfolded proteins (Seong *et al*., 2002).

The presence of the HslVU complex in bacteria and its absence in humans makes it an interesting drug target (Ramasamy *et al*., 2007;Tschan *et al*., 2010; Barboza *et al*., 2012; Kebe *et al*., 2019; Jeong *et al*., 2020; Singh *et al*., 2022). Small non-peptidic molecules belonging to different chemical scaffolds have been reported as activators of the HslV protease, which mimic the c-tail interaction pattern in binding with HslV dimer (Rashid *et al*., 2012). Previously, different coumarin derivatives have been identified to have antibacterial, antimicrobial, anticoagulant, anti-inflammatory, and antimalarial activities (Wu *et al*., 2009; Garg *et al*., 2020). Despite of great clinical significance, their mode of action has not been determined. During the present studies, the

*Corresponding authors: e-mails: yasmeen.rashid@uok.edu.pk; shahidbpk13@gmail.com

activation potential of 3-substituted coumarin derivatives against the HslV protease has been evaluated via both in-silico and in-vitro studies.

MATERIALS AND METHODS

Molecular docking studies

The three-dimensional structures of previously modeled HslV dimer (Rashid *et al*., 2012) and twenty-four derivatives of 3- substituted coumarin (ligands) were subjected to Auto dock Vina based docking studies (Trott and Olson, 2010). Marvin Sketch (Csizmadia, 1999) was utilized to draw the 3D structures of compounds. By using AUTODOCK tools (Dallakyan, 2010), files of both the receptor and compounds were prepared and saved in PDBQT format. DS visualizer (Visualizer, 2005) and VMD (Humphrey *et al*., 1996) were used for the detailed inspection of the three-dimensional docked complexes as well as to create their 2D images.

Experimental analysis of the HslV protease activation

In order to get the purified HslV protease, PET12b+ containing the HslV gene was transformed into BL21 codon plus (DE3) RIL cells. The HslV protease was expressed and purified as reported previously (Yoo *et al*, 1996; Bochtler *et al*., 1997). The peptide hydrolytic assay was carried out using the same reaction conditions as described previously (Rashid *et al*., 2012).The synthesis of these derivatives was reported previously (Salar *et al*., 2018). Compounds (codes: US-I-69, US-I-73, US-I-74) were tested for their HslV activation potential at five different concentrations i.e., 0.1, 0.25, 0.5, 1.0 and 1.5µM. The activation effect of synthetic HslU c-tail (ADEDLSRFIL) (AnaSpec. Inc. USA) was monitored as a control using the same experimental conditions. By observing constantly, the fluorescence of 7-amido-4-methyl coumarin (AMC) after its dissociation from Z-GGL-AMC fluorogenic peptide substrate at excitation λ =355nm and emission λ =460nm, the peptidase activity was assessed. The ED^{50} values (Effective concentration of the compound where half-maximal enzyme activation occurs) were calculated from the graphs of Vi\Vo versus the compound concentration where Vi and Vo were the velocities in the presence and absence of the compound. The Varioskan LUX 96 well plate reader (Thermo Scientific) along with SkanIt™ software for Microplate Readers version 6.0 was used to detect the AMC fluorescence in rfu (relative fluorescence unit).

Molecular dynamics simulations

The IMODS server (http://imods.chaconlab. org) was used to run molecular dynamics simulations in order to investigate the conformational stabilities of the interactions between the HslV-dimer and hit compounds using normal mode analysis (NMA) (López-Blanco *et al*., 2014).

STATISTICAL ANALYSIS

Standard deviation (SD) and Standard error of mean (SEM) were calculated using MS Office Excel 2016.

RESULTS

Molecular docking studies and analysis of protein-ligand interactions

The HslU c-tail, as well as 3-substituted coumarin derivatives, were docked well in the c-tail binding cleft of theHslV dimer (fig. 1B). In comparison with the HslU c-tail, all the twenty-four derivatives of this scaffold showed higher binding affinities towards the HslV c-tail binding pocket. Notably, US-I-74, US-I-73, and US-I-69 showed the binding affinities of -8.7, -8.5, and -8.3 kcal/mol which were quite higher than that of the HslU c-tail, i.e., -6.0 kcal/mol (table 1).

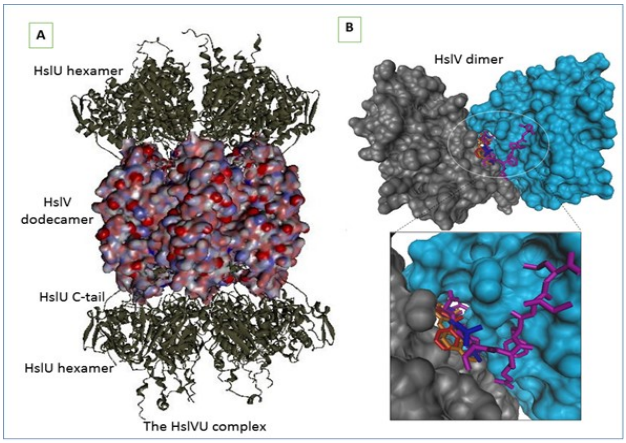

Fig. 1: (A) The overall three-dimensional structure of active HslVU complex, (B) HslV dimer complexed with docked ligands. In the closer view, the docked ligands in HslV c-tail binding pocket are shown in different colours, i.e., c-tail in magenta, US-I-74 in orange, US-I-73 in blue and US-I-69 in red.

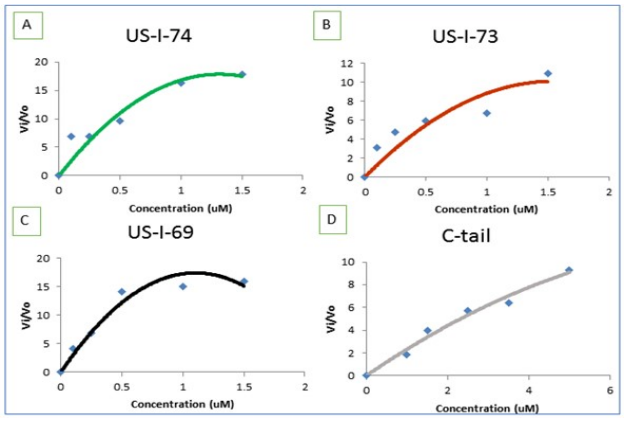

Fig. 2: *E. coli* HslV protease activation by different 3-substituted coumarin derivatives in a concentration-dependent manner.

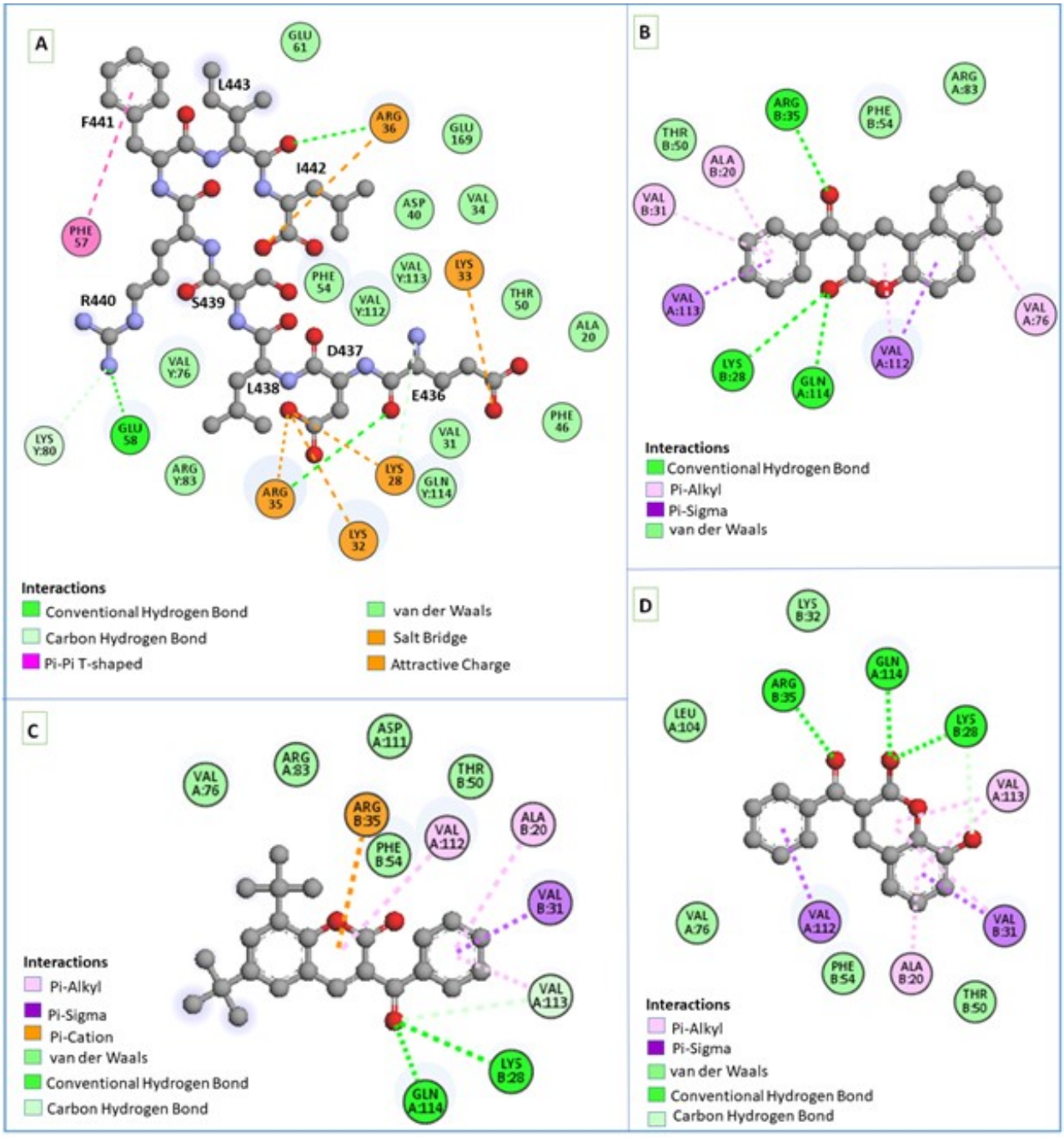

Fig. 3: Two-dimensional representations of intermolecular interactions between the HslV dimer and different activators; (A) c-tail (B) US-I-74, (C) US-I-73, and (D) US-I-69.

Detailed analysis of protein-ligand interactions revealed that the reference activator, i.e., HslU c-tail made several interactions with the crucial residues of the HslV dimer. The main interactions observed between the c-tail and the HslV dimer were five salt bridges with K28 (B), K32 (B), K33 (B), R35 (B), and R36 (B); three conventional hydrogen bonds with E58 (B), R35 (B) and R36 (B) residues of HslV dimer. The HslU c-tail was implicated in hydrophobic (π- π T-shaped and Vander Waals) contacts with twelve HslV residues, including four residues of subunit A (V112, V113, Q114, and V76) and eight residues (A20, V31, V34, F46, D40, F54, E61, and E169) of subunit B (Fig. 3A).

US-I-74 was proved to establish different hydrophilic and hydrophobic connections with the HslV dimer. K28 and R35 residues of the subunit B while Q114 residue of subunit Aformed three hydrogen bonds with this compound. V112 and V113 of subunit A made two π - sigma bonds; V76 and V112 of subunit A while A20 and

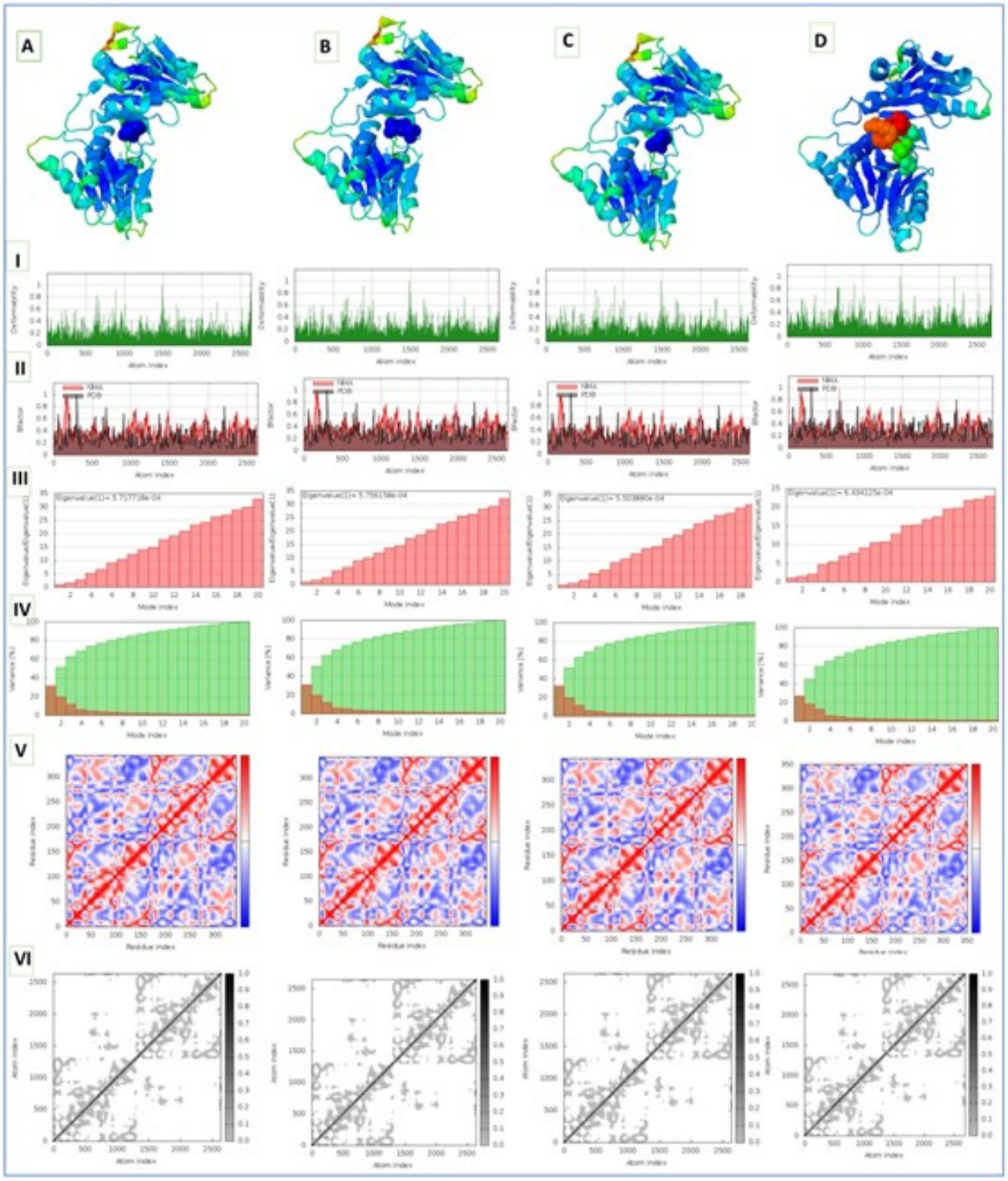

Fig. 4: Molecular dynamics simulation studies of HslV dimer-ligand docked complexes; (A) HslV-US-I-74, (B) HslV-US-I-73, and (C) HslV-US-I-73, (D) HslV-c-tail. The graphs illustrate (I) deformability, (II) B-factor, (III) eigenvalues, (IV) variance, (V) co-variance maps, and (VI) elastic network maps

V31 of subunit B were involved in making four π -alkyl. However, T50 and F54 residues of subunit B and R83of subunit A rendered the docked complex more stable by forming Vander Waals contacts with the ligand (fig. 3B).

A total of eleven residues made hydrophobic and hydrophilic bonds with US-I-73. The residues, i.e., K28 of subunit B and Q114 of subunit A, formed two hydrogen bonds;

Table 1: The codes, IUPAC names, and docking scores of 3-substituted coumarin derivatives

S. No.	Compound code	IUPAC Naming	Affinity kcal/mol
1	US-I-74	2-(phenylcarbonyl)-3*H*-benzo[*f*]chromen-3-one	-8.7
2	US-I-73	6,8-bis(1,1-dimethylethyl)-3-(phenylcarbonyl)-2*H*-chromen-2-one	-8.5
3	US-I-69	8-hydroxy-3-(phenylcarbonyl)-2*H*-chromen-2-one	-8.3
4	US-I-65	7-hydroxy-3-(phenylcarbonyl)-2*H*-chromen-2-one	-8.2
5	US-I-67	6,8-dichloro-3-(phenylcarbonyl)-2*H*-chromen-2-one	-8.0
6	US-I-71	3-(phenylcarbonyl)-2*H*-chromen-2-one	-8.0
7	US-I-75	6-hydroxy-3-(phenylcarbonyl)-2*H*-chromen-2-one	-8.0
8	US-I-68	8-bromo-6-chloro-3-(phenylcarbonyl)-2*H*-chromen-2-one	-8.0
9	US-I-62	7-(methyloxy)-3-(phenylcarbonyl)-2*H*-chromen-2-one	-7.9
10	US-I-64	6-chloro-3-(phenylcarbonyl)-2*H*-chromen-2-one	-7.9
11	US-I-66	6-fluoro-3-(phenylcarbonyl)-2*H*-chromen-2-one	-7.9
12	US-I-63	6-(methyloxy)-3-(phenylcarbonyl)-2*H*-chromen-2-one	-7.8
13	US-I-79	2-acetyl-3*H*-benzo[*f*]chromen-3-one	-7.5
14	US-I-82	3-acetyl-6,8-bis(1,1-dimethylethyl)-2*H*-chromen-2-one	-7.3
15	US-I-81	3-acetyl-6-fluoro-2*H*-chromen-2-one	-7.1
16	US-I-77	3-acetyl-6-chloro-2*H*-chromen-2-one	-7.0
17	US-I-76	3-acetyl-7-(methyloxy)-2*H*-chromen-2-one	-6.9
18	US-I-84	ethyl 7-(methyloxy)-2-oxo-2*H*-chromene-3-carboxylate	-6.8
19	US-I-80	3-acetyl-8-bromo-6-chloro-2*H*-chromen-2-one	-6.7
20	US-I-87	ethyl 6-fluoro-2-oxo-2*H*-chromene-3-carboxylate	-6.7
21	US-I-85	ethyl 6-(methyloxy)-2-oxo-2*H*-chromene-3-carboxylate	-6.5
22	US-I-91	ethyl 6-hydroxy-2-oxo-2*H*-chromene-3-carboxylate	-6.5
23	US-I-86	ethyl 6-chloro-2-oxo-2*H*-chromene-3-carboxylate	-6.4
24	US-I-88	ethyl 8-bromo-6-chloro-2-oxo-2*H*-chromene-3-carboxylate	-6.3

Table 2: Comparison of the docking scores, structures, and calculated ED^{50} values of the HslU c-tail and top-ranking 3-substituted coumarin derivatives

S. No.	Codes	Affinity kcal/mol	Structure	*E. coli* HslV Activation ED^{50}(μM)
1	HslU C-tail	-6.0	EDLSRFIL	2.6 ± 0.34
2	US-I-74	-8.7	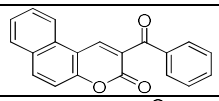	0.48 ± 0.052
3	US-I-73	-8.5	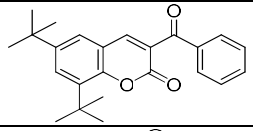	0.46 ± 0.186
4	US-I-69	-8.3	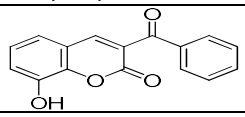	0.4 ± 0.080

±Standard Error of Mean

Whereas, R35 residue from subunit B made a single π -cationic bond The ligand also made three π -alkyl bonds with V112, V113 residues of subunit A and A20 residue of subunit B. V31 of subunit B and V113 of subunit A were observed to make a π -sigma and a carbon-hydrogen bond with the ligand, respectively. Three residues from subunit A including V76, R83, and D111, while two residues from subunit B including T50 and F54, together with keep this docked complex more stable by establishing Vander Waals connections with this ligand (fig. 3C).

US-I-69 interacted non-covalently with thirteen residues of the HslV dimer pocket. K28 and R35 residues from subunit B while Q114 from subunit A formed three hydrogen bonds; V112 of subunit A and V31 of subunit B formed two π -sigma bonds; A20 and V31 of subunit B and V31 of subunit B formed four π -alkyl bonds with this ligand.

Table 3: ADME properties of the identified lead molecules

S. No.	Properties	US-I-74	US-I-73	US-I-69
1	Molecular weight g/mol	300.31	362.46	266.25
2	No. of H-bond acceptor	4	3	4
3	No. of H-bonds donors	1	0	1
4	No. of rotatable bonds	5	4	2
5	Molar Refractivity	131.47	110.90	74.38
6	TPSA (Å²)	95.73	47.28	67.51
7	Solubility	-6.87 (poorly soluble)	-6.55 (poorly soluble)	-3.9 (soluble)
8	GI absorption	High	High	High
9	BBB permeant			
10	Log K_p(skin permeation)	-4.79	-5.43	-5.72
11	Consensus Log $P_{o/w}$	3.94	3.68	2.64
12	Lipinski			
13	Ghose			
14	Veber			
15	Egan			
16	Muegge			
17	Bioavailability score	0.55	0.55	0.55
18	Leadlikeness			
19	Synthetic accessibility	3.16	3.85	2.98

=Yes =No

Table 4: Predicted toxicity profile of 3-substituted coumarin derivatives

S. No	Parameters	US-I-74	US-I-73	US-I-69
1	0ral toxicity (mg/kg)	3000	3000	3000
2	Predicted toxicity class	Class 5	Class 5	Class 5
3	Average similarity (%)	73.19	71.97	73.94
4	Prediction Accuracy (%)	62.26	69.26	69.26
5	Organ toxicity (hepatotoxicity)	0.75 (inactive)	0.79 (inactive)	0.8 (inactive)
6	cytotoxicity	0.85 (inactive)	0.66 (inactive)	0.72 (inactive)
7	PPAR. Gamma	0.90 (inactive)	0.94 (inactive)	0.84 (inactive)
8	Phosphoprotein tumor suppressor p53	0.89 (inactive)	0.70 (inactive)	0.79 (inactive)

However, vander Waals contacts were furnished by two residues, i.e., L104 and V76 from subunit A and three residues, i.e., K32, F54, and T50 from subunit B (fig. 3D).

Fluorescence-based HslV activation assay

The HslU c-tail and 3-substituted coumarin derivatives were observed to significantly activate the HslV protease in a concentration-dependent manner even in the absence of its natural activator, i.e., HslU (fig. 2). The calculated ED^{50} value for the c-tail was found to be 2.6 ± 0.34µM. Although, ED^{50} values for these potential hits were observed to be much lower, i.e., 0.48 ± 0.052 µM for US-I-74, 0.46 ± 0.186µM for US-I-73, and 0.4 ± 0.080 µM for US-I-69 (table 2).

Molecular dynamics simulation results

The normal mode analysis (NMA) of the docked complexes was performed using the IMODS server [López-Blanco *et al*., 2014] to define their molecular flexibility**.** The deformability graphs (fig. 4I) of the docked complexes demonstrated the ability of each molecule to deform at each of its residues. The B-factor graphs of the complexes (fig. 4II) represented a comparison of the docked complexes' NMA and PDB

fields. The motion stiffness was determined by the computed eigenvalues of the docked complexes (fig. 4III). The calculated eigenvalue of the HslVdimer/ US-I-74 complex was 5.717718e-04, HslVdimer/US-I-73 complex was 5.756158e0-4, and HslVdimer/US-I-69 was5.50388e0-4. However, the computed eigenvalue of the HslVdimer/c-tail complex is 6.434125e-04. Each normal mode's associated variance is inversely proportional to its eigenvalue. Individual variance is shown by red bars, while cumulative variance is represented by green bars (fig. 4IV). A co-variance map depicts coupling between the pairs of residues, with red, white, and blue colors indicating correlated, uncorrelated, and anti-correlated motion, respectively (fig. 4V). The elastic networks of complexes are displayed by elastic maps (fig. 4VI), which highlight the connection between pairs of atoms through springs. Each dot signifies one spring between the atomic pairs it represents. Spring stiffness is indicated by darker spots and vice versa.

In silico assessment of the drug-like properties of lead molecules

The fate of a therapeutic molecule in an organism is determined by a number of factors that influence target access. Computational approaches can be used to evaluate parameters like absorption, distribution, metabolism, and excretion (Daina *et al*., 2017). The ADME profiles of hit compounds were investigated using a web tool Swiss ADME (http://www.swissadme.ch/). Whereas, ProTox-II (https://tox-new.charite.de/protox_II) was used to predict the in-silico toxicity prediction. The molecular weights of the compounds were all less than 500g/mol. These three ligands showed TPSA values that were substantially lower than 150. When the LogP values of all the ligands were compared, it is clear that none of them have more than 5. These positive outcomes demonstrated the body's ability to absorb easily. The ligand US-I-69 is soluble, but US-I-74 and US-I-73 are not. In addition, ligands have a high GI absorption (table 3). All of the compounds have less than five hydrogen bond donors and fewer than ten hydrogen bond acceptors. All ligands have molar refractivity values less than 130. The Lipinski rule of Five, Veber, and Egan were strictly followed by all of the ligands. Both US-I-74 and US-I-69 obeyed the other two rules, namely Ghose and Muegge, while US-I-73 did not (table 3). These positive outcomes demonstrated the compound's ability to absorb easily.

Table 4 shows the toxicity profile of active coumarin derivatives. The toxicity of these active compounds is measured in terms of toxicity endpoints (cytotoxicity). It can also be quantified qualitatively, such as binary (active or inactive) for specific cell kinds and assays, or quantitatively, such as LD50 (fatal dosage) values, for particular cell types and assays, or indication areas such as cytotoxicity, hepatotoxicity, PPAR. Gamma and phosphoprotein tumor suppressor p53 (Banerjee *et al*., 2018).

DISCUSSION

The growing antibiotic resistance in pathogenic bacteria is a risk to the public health globally which alarms the effectiveness of existing medicine (Wernli *et al*., 2017). Therefore, there is an emergent need for the development or identification of new drug candidates with potential antimicrobial properties and novel modes of action.

Clp proteases in bacteria are required for protein turnover and homeostasis as well as to perform crucial physiological functions. Owing to their apparent essentiality in numerous cellular functions, these proteases gained a lot of attention as an antibacterial target in recent years (Brötz-Oesterhelt and Sass, 2014). To date, all the antibiotics in therapeutic applications tend to inhibit bacterial growth using the target inactivation mechanism. However, a novel concept to disrupt the pathogenic microbes by over-activating rather than inhibiting the target enzyme complex has been in practice for the last few years. Acyldepsipeptides (ADEPs) have been proven as potent antibiotics that activate ClpP and cause aberrant proteolysis, which limits the bacterial cell division and eventually leads to cell death (Moreno-Cinos *et al*., 2019; Gersch *et al*., 2015). Likewise, the HslVU complex, also known as ClpQY (Ramachandran *et al*., 2002), which plays a key role in maintaining the essential bacterial proteostasis, is an attractive antibacterial drug target. Similar to clpP, the over-activation of HslV protease has also been related to uncontrolled protein degradation within the pathogen leading to its death. Fewer studies have been reported that were focused on the over-activation of the HslV protease to impair the growth of pathogenic microbes by identifying specific non-peptidic or peptidic activators. These molecules are considered to mimic the HslU c-tail in interacting and activating the HslV protease (Rashid *et al*., 2012; Kebe *et al*., 2019). Recently, it has been proved that uncontrolled HslV activation leads to parasitic growth inhibition (Singh *et al*., 2022).

The present study aimed to identify active compounds having coumarin scaffold via both in-silico and in-vitro studies that have the potential to over-activate the HslV protease even at lower concentrations. Due to the unavailability of the crystal structure of active *E. coli* HslVU complex (fig. 1A), the previously constructed model of *E. coli* HslV dimer complexed with the HslUc-tail was used for molecular docking studies (Rashid *et al*., 2012). The docking results showed comparatively lower energies and, hence, better binding affinities of these 3-substituted coumarin derivatives than that of thec-tail. Consistently, these compounds showed concentration-dependent activation of the HslV protease in the absence of its natural activator (HslU c-tail). The effective doses (concentrations) of the top three compounds (i.e. ED^{50}) were in the range of 0.4-0.48 µM, which were lesser than

that of the c-tail, i.e., 2.6µM under the same experimental conditions (table 2). These results revealed that these compounds harbor more potential to activate the HslV protease than its natural activator.

Thorough comparative analysis of the docked complexes revealed that the interaction behaviors of the c-tail and the lead compounds differ only slightly. Although the HslU c-tail was comparatively larger than the chemical compounds and showed to make more interactions with the HslV dimer, the critical interactions including hydrogen bonds and hydrophobic forces were all very similar. However, the three chemical compounds also showed other distinctive interactions with HslV dimeric crevice including π-alkyl and π-sigma bonds, which were mediated by their intrinsic lactone ring. Notably, the lactone ring is an already known structural entity for maintaining various activities (Pangal *et al*., 2013). Structurally coumarins are bicyclic lactones and their derivatives have been reported to have diverse biological functions including antibacterial, antimicrobial, anticoagulant, anti-inflammatory, and antimalarial activities (Wu *et al*., 2009; Garg *et al*., 2020). In addition, the derivatives of this scaffold are potent inhibitors of DNA gyrase which plays an essential role in cell growth (Kalkhambkar *et al*., 2008). Consistently, the antibacterial activity against the gram-positive bacteria (multidrug-resistant *staphylococcus aureus*) of coumarin derivatives is already reported (Salar *et al*., 2018). Regardless of their importance, their mode of action is still not known.

During the present studies, these hit molecules were found to be efficiently fixed in the HslV dimer's c-tail binding pocket regardless of possessing smaller structures than the HslU c-tail and capable of intensifying HslV protease activity several folds (table 2). Distinct substitutions on their lactone rings are responsible for the slight differences in their activation potentials. According to molecular dynamics simulations, all the identified hit molecules have lower eigen values than the c-tail (fig. 4), implying that these active ligands require less energy to distort the HslV dimeric structure. ADMET (table 3 and 4) findings further suggested that all the three derivatives have a strong drug-like profile and are incredibly safe to use. US-I-74 and US-I-69, on the other hand, demonstrated to have a more promising ADME profile (table 3). The predicted lethal dose of these derivatives is 3000 mg/kg and all of them belong to class 5 with an average similarity range of 71.94-73.94% and having prediction accuracy range of 62.26-69.26%. Furthermore, all three hits are also safe for liver health, non-cytotoxic, and also inactive for the receptors PPAR. Gamma and phosphoprotein tumor suppressor p53 (table 4). These favorable results further validate that these synthetic HslV protease activators possess the potential to become active and safe anti-microbial drugs.

CONCLUSION

The importance of protein-ligand interactions and the MD simulation method in identifying possible therapeutic candidates is an already established strategy (Aurangzeb *et al*., 2018; Hamid *et al*., 2021; Hunanyan *et al*., 2021; Singh *et al*., 2022). The utilization of molecular docking techniques makes it easier to comprehend the mode of action of chemical molecules that may interact with the target (Meng *et al*., 2011). The present research revealed the significance of molecular docking studies in the selection of the best hits based on their least binding energies whereas the ligand interaction and simulation analysis demonstrated the noteworthy indication of the structural and chemical association of these derivatives with the c-tail pocket of HslV dimer. The HslV activation assay further validated that these compounds have potential to activate HslV protease with ED^{50} values even lower than HslU c-tail. We believe that these compounds are likely to be good hit to lead molecules for designing effective antimicrobial drug which can initiate uncontrolled proteolysis in microbes via a unique mode of antibacterial mechanism.

ACKNOWLEDGMENTS

We are grateful to Higher Education Commission (HEC), Pakistan for financial support under National Research Program for Universities (NRPU)-2014 (Project No. 20-4102). We also owe a debt of gratitude to Professor Robert T. Sauer, Department of Biology, Massachusetts Institute of Technology, USA, for the providing of the HslV gene containing the PET12b+ vector.

REFERENCES

Aurangzeb S, Hamid M, Rashid Y, Hameed A and Khan KM (2018). Three dimensional structural investigation of lead molecules against neisseria meningitis pathogenic factors; A step towards drug designing. *PJBMB*, **51**(1-2): 31-56.

Azim MK (2021). Structure of prokaryotic HslVU protease-chaperone complex. *PJBMB,* **54**(1-2): 6-13.

Azim MK, Goehring W, Song HK, Ramachandran R, Bochtler M and Goettig P (2005). Characterization of the HslU chaperone affinity for HslV protease. *Protein Sci,* **14**(5): 1357-1362.

Banerjee P, Eckert AO, Schrey AK and Preissner R (2018). ProTox-II: A webserver for the prediction of toxicity of chemicals. *Nucleic Acids Res,* **46**(1): 257-263.

Barboza NR., Cardoso J, de Paula Lima CV, Soares MJ, Gradia DF, Hangai NS, Bahia MT, de Lana M, Krieger MA and de Sa RG (2012). Expression profile and subcellular localization of HslV, the proteasome related protease from Trypanosomacruzi. *Exp. Parasito,* **130**(2): 171-177.

Bochtler M, Ditzel L, Groll M and Huber R (1997). Crystal structure of heat shock locus V (HslV) from *Escherichia coli*. *Proc. Natl. Acad. Sci. U.S.A,* **94**(12): 6070-6074.

Brotz-Oesterhelt H and Sass P (2014). Bacterial caseinolytic proteases as novel targets for antibacterial treatment. *Int. J. Med. Microbiol,* **304**(1): 23-30.

Csizmadia P (1999). MarvinSketch and MarvinView: molecule applets for the World Wide Web.

Daina A, Michielin O and Zoete V (2017).SwissADME: a free web tool to evaluate pharmacokinetics, drug-likeness and medicinal chemistry friendliness of small molecules. *Sci. Rep,* **7**(1): 1-13.

Dallakyan S (2010). MGLTools. *Reference Source*.

Garg SS, Gupta J, Sharma S and Sahu D (2020).An insight into the therapeutic applications of coumarin compounds and their mechanisms of action. *Eur. J. Pharm. Sci.,* **152**: 105424.

Gersch M, Famulla K, Dahmen M, Gobl C, Malik I, Richter K, Korotkov VS, Sass, P, Rubsamen-Schaeff H, Madl T and Brotz-Oesterhelt H (2015). AAA+ chaperones and acyldepsipeptides activate the ClpP protease via conformational control. *Nat. Commun.,* **6**(1): 1-12.

Hamid M, Aurangzeb S, Rashid Y, Khan KM and Hameed A (2021). Identification and structural investigation of potential novel drug candidates against lethal human pathogen. *Pak. J. Pharm. Sci.,* **34**(1): 21-34.

Humphrey W, Dalke A and Schulten K (1996). VMD: visual molecular dynamics. *J. Mol. Graph.,* **14**(1): 33-38.

Hunanyan L, Ghamaryan V, Makichyan A and Popugaeva E (2021). Computer-based drug design of positive modulators of store-operated calcium channels to prevent synaptic dysfunction in Alzheimer's disease. *Int. J. Mol. Sci.,* **22**(24): 13618.

Jeong S, Ahn J, Kwon AR and Ha NC (2020). Cleavage-dependent activation of ATP-dependent protease HslUV from *Staphylococcus aureus. Mol. Cells,* **43**(8): 694.

Kalkhambkar RG, Kulkarni GM, Kamanavalli CM, Premkumar N, Asdaq SMB and Sun CM (2008). Synthesis and biological activities of some new fluorinated coumarins and 1-aza coumarins. *Eur. J. Med. Chem.,* **43**(10): 2178-2188.

Kebe NM, Samanta K, Singh P, Lai-Kee-Him J, Apicella V, Payrot N, Lauraire N, Legrand B, Lisowski V, Mbang-Benet DE and Pages M (2019). The HslV protease from Leishmania major and its activation by C-terminal HslU peptides. *Int. J. Mol. Sci.,* **20**(5): 1021.

Lopez-Blanco JR, Aliaga JI, Quintana-Ortí, ES and Chacon P (2014). iMODS: internal coordinates normal mode analysis server. *Nucleic Acids Res.,* **42**(1): 271-276.

Meng XY, Zhang HX, Mezei M and Cui M (2011). Molecular docking: A powerful approach for structure-based drug discovery. *Curr. Comput. Aided Drug Des.,* **7**(2): 146-157.

Missiakas D, Schwager F, Betton JM, Georgopoulos C and Raina S (1996). Identification and characterization of HsIVHsIU (ClpQClpY) proteins involved in overall proteolysis of misfolded proteins in *Escherichia coli*. *EMBO J,* **15**(24): 6899-6909.

Moreno-Cinos C, Goossens K, Salado IG, Van Der Veken P, De Winter H and Augustyns K (2019).ClpP protease, a promising antimicrobial target. *Int. J. Mol. Sci.,* **20**(9): 2232.

Pangal A, Gazge M, Mane V and Shaikh JA (2013). Various pharmacological aspects of coumarin derivatives: A review. *IJPRBS*, **2**(6): 168-194.

Park E, Lee JW, Eom SH, Seol JH and Chung CH (2008). Binding of MG132 or deletion of the Thr active sites in HslV subunits increases the affinity of HslV protease for HslU ATPase and makes this interaction nucleotide-independent. *J. Biol. Chem.,* **283**(48): 33258-33266.

Ramachandran R, Hartmann C, Song, HK, Huber R and Bochtler M (2002).Functional interactions of HslV (ClpQ) with the ATPase HslU (ClpY). *Proc. Natl. Acad. Sci. U.S.A*, **99**(11): 7396-7401.

Ramasamy G, Gupta D, Mohmmed A and Chauhan VS (2007). Characterization and localization of *Plasmodium falciparum* homolog of prokaryotic ClpQ/HslV protease. *Mol. Biochem. Parasitol.,* **152**(2): 139-148.

Rashid Y, Azim MK, Saify, ZS, Khan KM and Khan R (2012). Small molecule activators of proteasome-related HslV peptidase. *Bioorg. Med. Chem. Lett.,* **22**(19): 6089-6094.

Salar U, Khan, KM, Muhammad H, Fakhri MI, Perveen S and Choudhary MI (2018). Anti-MRSA (Multidrug resistant *Staphylococcus aureus*) activity of 3-substituted coumarins. *Lett. Drug Des. Discov.,* **15**(4): 353-362.

Seong IS, Kang MS, Choi, MK, Lee, JW, Koh OJ, Wang J, Eom, SH and Chung CH (2002). The C-terminal tails of HslU ATPase act as a molecular switch for activation of HslV peptidase. *J. Biol. Chem.,* **277**(29): 25976-25982.

Singh P, Samanta K, Kebe NM, Michel G, Legrand B, Sitnikova VE, Kajava AV, Pages M, Bastien P, Pomares C and Coux O (2022). The C-terminal segment of Leishmania major HslU: Toward potential inhibitors of LmHslVU activity. *Bioorg. Chem.,* **119**: 105539.

Singh G, Soni H, Tandon S, Kumar V, Babu G, Gupta V and Chaudhuri P (2022). Identification of natural DHFR inhibitors in MRSA strains: Structure-based drug design study. *Results Chem,* **4**: 100292.

Sousa MC, Trame CB, Tsuruta H, Wilbanks SM, Reddy VS and McKay DB (2000).Crystal and solution structures of an HslUV protease-chaperone complex. *Cell*, **103**(4): 633-643.

Trott O and Olson AJ (2010). AutoDockVina: Improving the speed and accuracy of docking with a new scoring

function, efficient optimization, and multithreading. *J. Comput. Chem.,* **31**(2): 455-461.

Tschan S, Kreidenweiss A, Stierhof YD, Sessler N, Fendel R and Mordmüller B (2010). Mitochondrial localization of the threonine peptidase PfHslV, a ClpQortholog in *Plasmodium falciparum*. *Int. J. Parasitol.,* **40**(13): 1517-1523.

Visualizer DS (2005). Accelrys Software Inc. Discovery Studio Visualizer, 2.

Wernli D, Jørgensen PS, Harbarth S, Carroll SP, Laxminarayan R, Levrat N, Røttingen JA and Pittet D (2017). Antimicrobial resistance: The complex challenge of measurement to inform policy and the public. *PLoS Med.,* **14**(8): 1002378.

Wu L, Wang X, Xu W, Farzaneh F and Xu R (2009).The structure and pharmacological functions of coumarins and their derivatives Curr. *Med. Chem.,* **16(**32): 4236-4260.

Yoo SJ, Seol JH, Shin DH, Rohrwild M, Kang MS, Tanaka K, Goldberg AL and Chung CH (1996). Purification and characterization of the heat shock proteins HslV and HslU that form a new ATP-dependent protease in *Escherichia coli. J. Biol. Chem.,* **271**(24): 14035-14040.